





RESEARCH ARTICLE

Supramolecular interactions between β -lapachone with cyclodextrins studied using isothermal titration calorimetry and molecular modeling

Francisco H. Xavier-Junior¹  | Marcelo M. Rabello² | Marcelo Z. Hernandez²  |
Marília E.S. Dias¹ | Otoni H.M.S. Andrada¹ | Beatriz P. Bezerra³ | Alejandro P. Ayala³  |
Nereide S. Santos-Magalhães¹ 

¹Laboratório de Imunopatologia Keizo-Asami, Universidade Federal de Pernambuco (UFPE), Recife, PE, Brazil

²Departamento de Ciências Farmacêuticas, Laboratório de Química Teórica Medicinal, Universidade Federal de Pernambuco, Recife, PE, Brazil

³Departamento de Física, Universidade Federal do Ceará, Fortaleza, CE, Brazil

Correspondence

Nereide S. Santos-Magalhães, Laboratório de Imunopatologia Keizo-Asami (LIKA), Universidade Federal de Pernambuco (UFPE), Av. Prof. Moraes Rego, 1235, Cidade Universitária, Recife 50670-901, PE, Brazil. Email: nssm@ufpe.br

Funding information

CAPES; National Council for Research and Development of Brazil (CNPq), Grant/Award Number: 311232/2013-2 and 402282/2013-2; Fundação de Amparo à Ciência e Tecnologia do Estado de Pernambuco (FACEPE), Grant/Award Number: APQ-1868-4.03/13; Brazilian Ministry of Science and Technology

Abstract

Supramolecular interactions between β -lapachone (β -lap) and cyclodextrins (CDs) were investigated by isothermal titration calorimetry. The most favorable host: guest interaction was characterized using X-ray powder diffraction (XRD), differential scanning calorimetry and thermogravimetry (DSC/TG), spectroscopy (FT-IR), spectroscopy (2D ROESY) nuclear magnetic resonance (NMR), and molecular modeling. Phase solubility diagrams showed β -, HP- β -, SBE- β -, γ -, and HP- γ -CDs at 1.5% (w/w) allowed an increase in apparent solubility of β -lap with enhancement factors of 12.0, 10.1, 11.8, 2.4, and 2.2, respectively. β -lap has a weak interaction with γ - and HP- γ -CDs and tends to interact more favorably with β -CD and its derivatives, especially SBE- β -CD ($K = 4160 \text{ M}^{-1}$; $\Delta G = -20.66 \text{ kJ}\cdot\text{mol}^{-1}$). Thermodynamic analysis suggests a hydrophobic interaction associated with the displacement of water from the cavity of the CD by the β -lap. In addition, van der Waals forces and hydrogen bonds were responsible for the formation of complexes. Taken together, the results showed intermolecular interactions between β -lap and SBE- β -CD, thereby confirming the formation of the inclusion complex. Molecular docking results showed 2 main orientations in which the interaction of benzene moiety at the wider rim of the SBE- β -CD is the most stable (average docking energy of -7.0 kcal/mol). In conclusion, β -lap: SBE- β -CD is proposed as an approach for use in drug delivery systems in cancer research.

KEYWORDS

cyclodextrins, isothermal titration calorimetry, molecular modeling, phase solubility, β -lapachone

1 | INTRODUCTION

β -lapachone (3,4-dihydro-2,2-dimethyl-2H-naphthol-[1,2-b]pyran-5,6-dione) is a naphthoquinone derived from the lapachol, which is isolated

Chemical compounds studied in this article: β -lapachone (PubChem CID: 3885); Sulfobutyl ether- β -cyclodextrin (PubChem CID: 44296702); β -cyclodextrin (PubChem CID: 444041); 2-hydroxypropyl- β -cyclodextrin (PubChem CID: 44134771); γ -cyclodextrin (PubChem CID: 5287407).

Abbreviations: CD, cyclodextrin; CE, complexation efficiency; DS, degree of substitution per glucose unit; HP- β -CD, 2-hydroxypropyl- β -cyclodextrin; HP- γ -CD, 2-hydroxypropyl- γ -cyclodextrin; ITC, isothermal titration microcalorimetry; K, binding constant; $K_{1:1}$, apparent stability constant; n, stoichiometry of the interaction; SBE- β -CD, sulfobutyl ether- β -cyclodextrin; β -CD, β -cyclodextrin; β -lap, β -lapachone (3,4-dihydro-2,2-dimethyl-2H-naphthol-[1,2-b]pyran-5,6-dione); γ -CD, γ -cyclodextrin; ΔG , Gibbs free energy; ΔH , change in enthalpy; ΔS , change in entropy

from the bark of the *Tabebuia avellanedae*, a tree native to South America.¹ β -lapachone (β -lap) presents several pharmacological properties including antineoplastic activity.²⁻⁸ The mechanism of action of the β -lap involves an increased generation of reactive oxygen species, inducing extensive DNA damage, H2AX phosphorylation, and Poly (ADP ribose) polymerase hyperactivation culminating in apoptosis. In addition, the main advantage of β -lap over other antineoplastic agents is the induction of apoptosis in a nondependent activity of p53/p21, cell cycle state or caspases.^{9,10} Despite its potential pharmacological activities, β -lap has limited use because of its low solubility in water (0.16 mM),^{11,12} which makes attaining the plasma levels needed for optimal therapeutic efficacy problematic. To overcome this limitation, cyclodextrins (CDs) can be used to increase the solubility and bioavailability of β -lap as inclusion complexes.

The CDs often improve the solubility, stability, and consequently the bioavailability of the guest drug inserted into their cavities.^{13–17} The coexistence of multiple inclusion modes of the guest molecules into the CD cavity has been reported in the literature. Generally, the complexation of the drugs depends largely on the hydrophobicity and geometry of the guest molecule, the physicochemical properties of the CD (size of CD cavity, outer hydrophilicity), as well as the method and variables involved in the complex production process (kneading, freeze drying, temperature, and pH).^{17,18} The driving forces are both Van der Waals interactions, as well as the possible hydrophobic effect and hydrogen bonding at the rim of the cavity.^{19,20}

Several approaches have been used based on the use of inclusion complexes of β -lap with CDs to increase its solubility.^{11,12,21,22} However, these studies have been limited to the thermodynamic profile analysis of the interaction between β -lap and CD. To our knowledge, β -lap with native CDs inclusion complexes have been successfully developed in previous studies but not yet applied to sulfobutyl ether- β -CD (SBE- β -CD). In the present study, a careful physicochemical characterization of this supramolecular complex stoichiometry, binding sites, and three-dimensional arrangements were investigated to provide highly important information for choosing the best drug: CD ratio, which might lead to a better drug activity. To this end, the thermodynamic parameters of interactions between β -lap and CDs were measured by isothermal titration microcalorimetry (ITC), varying the CD cavity size (β - and γ -CDs), and highly water-soluble chemically substituted CDs: hydroxypropyl- β -CD (HP- β -CD), SBE- β -CD, and hydroxypropyl- γ -CD (HP- γ -CD) to identify the best CD capable of improving β -lap aqueous solubility (Figure 1 and Table 1). The most favorable

supramolecular complex was thus characterized using thermal and spectroscopic analyses and molecular modeling.

2 | MATERIAL AND METHODS

2.1 | Materials

β -lapachone (β -lap), obtained from lapachol by a semisynthetic route, was supplied by Dr Alexandre Goes (UFPE, Brazil). Sulfobutyl ether- β -cyclodextrin (SBE- β -CD) (Captisol) with a degree of substitution (DS) per glucose unit of 0.9 was a gift from CyDex Pharmaceuticals (Kansas). β -cyclodextrin (β -CD), 2-hydroxypropyl- β -cyclodextrin (HP- β -CD); DS = 0.6, γ -cyclodextrin (γ -CD), 2-hydroxypropyl- γ -cyclodextrin (HP- γ -CD) DS = 0.6, methanol HPLC grade, sodium phosphate dibasic, sodium phosphate monobasic, trifluoroacetic acid, potassium bromide (KBr), sodium 3-(trimethylsilyl) propionate- d_4 (99%), and deuterium oxide (D_2O) (99.96%) were purchased from Sigma-Aldrich (St. Louis, Missouri). All chemicals were of analytical or reagent grade and were used without further purification. Ultrapure water was obtained from a water purification system (Milli-Q plus, Millipore, Billerica, Massachusetts) with resistivity and total organic carbon of 16.3 M Ω cm and 2 ppm at 25°C, respectively. Phosphate buffer solutions (0.05 M) at pH 7.4 were prepared according USP 34th edition.

2.2 | Phase solubility diagrams and apparent aqueous solubility

Phase-solubility studies were performed according to the method reported by Higuchi and Connors.²³ To confirm the effect of CDs (β -, HP- β -, SBE- β -, γ -, and HP- γ -CD) on the aqueous solubility of β -lap,

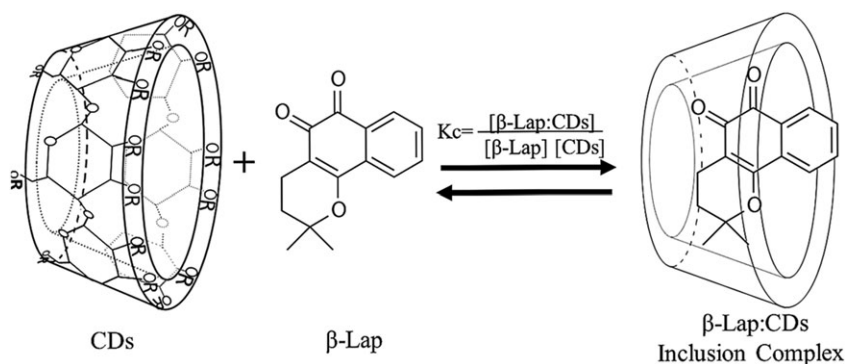


FIGURE 1 Equilibrium constant of chemical interaction between β -lap in aqueous solutions containing CDs for formation of inclusion complex. $[\beta\text{-lap:CD}]$, $[\beta\text{-lap}]$, and $[CD]$ are the concentrations of inclusion complex of β -lap and CD, free β -lap, and free CD, respectively. R corresponds to the radical present in different CD structures according Table 1

TABLE 1 General molecular characteristics and physicochemical proprieties of the CDs

Type of Cyclodextrin	Abbreviation	R ^a	Glucose Units	Cavity Diameter (Å)	Aprox. Volume Cavity (Å ³)	Molecular Weight ^c (g·mol ⁻¹)	Solub. in Water at 25°C (%w/w)
β -Cyclodextrin	β -CD	H	7	6.0–6.5	262	1135	1.85
γ -Cyclodextrin	γ -CD	H	8	7.5–8.3	427	1297	23.2
(2-Hydroxypropyl)- β -Cyclodextrin	HP- β -CD	CH ₂ CHOCH ₃	7	Variable	Variable	1380 ^b	>60
Sulfobutyl ether- β -cyclodextrin	SBE- β -CD	(CH ₂) ₄ SO ₃ Na	7	Variable	Variable	2163 ^b	>90
(2-Hydroxypropyl)- γ -Cyclodextrin	HP- γ -CD	CH ₂ CHOCH ₃	8	Variable	Variable	~1580	>50

^aSee the structure above.

^bMean value, depending on the substitution degree of CD.

^cMW provided by the supplier.

an excess of the drug was placed in a glass vial with 2 mL of solubilizing agent in phosphate buffer (0.05 M, pH = 7.4) at 25°C. The CDs were used at concentrations ranging from 0.5% to 40% w/w for HP- β -CD, SBE- β -CD, and HP- γ -CD, from 0.5% to 20% (w/w) for γ -CD and from 0.3% to 1.8% (w/w) for β -CD, because of its aqueous solubility limitations at 25°C (Table 1). Vials containing an excess of β -lap dispersed in a solution of CD were sealed, protected from light, and shaken by magnetic stirrer at 300 rpm (C-MAG HS 7 IKA, Staufen, Germany) for 24 hours at $25 \pm 1^\circ\text{C}$. After equilibration, samples were centrifuged at 8792 g for 15 minutes (Kubota KR-20000 T, Rotor RA-1 M, Tokyo, Japan) to remove insoluble crystals of β -lap and the supernatants filtered through a 0.22- μm membrane filter (Millex, Millipore, France). The filtrates were then diluted as required with the mobile phase and placed in an ultrasound bath (Unique USC-750, São Paulo, Brazil) for 5 minutes. The high performance liquid chromatography (HPLC) method was used to analyze β -lap concentration. The solubility of β -lap in water was determined in the absence of CDs.

The phase solubility diagrams were obtained by plotting the β -lap concentration as a function of CDs molar concentrations. The apparent stability constant ($K_{1:1}$) was then calculated from the slope of the phase-solubility diagrams assuming a 1:1 ratio of complex formation using Equation 1:

$$K_{1:1} = \frac{\text{Slope}}{S_0 (1 - \text{Slope})} \quad (1)$$

The slope was obtained by linear regression fitting the initial straight-line portion of the plot of β -lap concentration against CDs concentration, and S_0 was the solubility of β -lap in water in the absence of CD.

The complexation efficiency (CE) of β -lap was determined from data of the phase-solubility curve according to Equation 2:

$$\text{CE} = \frac{\text{Slope}}{1 - \text{Slope}} \quad (2)$$

2.3 | HPLC determination of β -lap concentration

Samples containing β -lap were analyzed using an HPLC system (Alliance 2695, Waters, Milford, Massachusetts) coupled to the photodiode array 2998. Chromatographic separations were achieved using a reversed-phase column C18 (250 mm \times 4.6 mm, 5 μm , XBridge Waters). The detection wavelength was set at 256 nm, which was the maximum absorbance level observed for β -lap. The mobile phase consisting of an isocratic mixture of methanol: 0.05% trichloroacetic acid aqueous solution (70:30, v/v, pH = 2.0) was pumped through the column at a flow rate of 0.9 mL \cdot min $^{-1}$ at 37°C. The 50- μL samples were injected into the HPLC system every 12 minutes. The mobile phase and the samples were filtered (0.22- μm filters, Millipore, Massachusetts) prior to use. Data acquisition and processing were performed using Empower automation system software.

β -lap concentrations in the inclusion complexes (β -CD, HP- β -CD, SBE- β -CD, γ -CD, and HP- γ -CD) were obtained using the linear regression equation ($\text{Abs} = 332\,787 [\beta\text{-lap}] + 18\,840$, $R^2 = 0.999$) from the fitted β -lap standard curve prepared with concentrations ranging from 1 to 80 $\mu\text{g}\cdot\text{mL}^{-1}$.

2.4 | Isothermal titration calorimetric studies

The energy of the binding of the β -lap with CDs (β -CD, HP- β -CD, SBE- β -CD, γ -CD, and HP- γ -CD) was studied using an isothermal titration calorimeter (ITC-200 MicroCal/GE, Northampton, Massachusetts) periodically calibrated either electrically using an internal electric heater or chemically by measuring the dilution enthalpy of methanol in water. For the ITC experiments, β -lap (0.16 mM) solution was prepared dissolving an excess of β -lap (5 mg) in a glass vial with 50 mL of phosphate buffer (0.05 M, pH = 7.4) under magnetic stirring 500 rpm for 24 hours at $25 \pm 1^\circ\text{C}$. A yellowish dispersion obtained was centrifuged at 8792 g for 15 minutes (Kubota KR-20 000 T centrifuge, Rotor RA-1 M, Tokyo, Japan) and the supernatant filtered through a 0.22- μm membrane filter (Millex, Millipore, France). All titrant solutions of CDs at 1.5% (w/w) were prepared in phosphate buffer (0.05 M, pH 7.4) corresponding to molar concentrations of 13.22, 10.87, 6.93, 11.57, and 9.49 mM to β -CD, HP- β -CD, SBE- β -CD, γ -CD, and HP- γ -CD, respectively. Prior to each experiment, all solutions (β -lap and CDs) were filtered through a 0.22- μm membrane (Millex, Millipore, France) and degassed using an ultrasound bath (Unique USC-750, São Paulo, Brazil) for 30 minutes. The sample cell was filled with 200 μL of β -lap solution (0.16 mM) and titrated with 40 μL of CD solution placed in the stirring syringe. The first injection of 0.4 μL was discarded to eliminate diffusion effects of material from the syringe to the sample cell. Experiments were planned to consist of 20 consecutive injections (2 μL) with a duration of 5 seconds each with intervals of 180 seconds at a stirring speed of 350 rpm at 25°C. The values of heat capacity of binding were adjusted considering the dilution effects of CD solubilized in buffer solution placed in the sample cell. Data consisted of a series of heat flows as a function of time. The interaction process between the 2 species was analyzed by means of a one-site binding model (Origin 7 software). On the basis of the concentrations of the titrant and the sample, the software used a non-linear least-squares algorithm (minimization of χ^2) to fit the series of heat flows (enthalpograms) to an equilibrium binding equation, providing the best fit values of the stoichiometry of the interaction (n), binding constant (K), change in enthalpy (ΔH), and entropy (ΔS). The Gibbs free energy (ΔG) was calculated on the basis of Equation 3:

$$\Delta G = -R T \ln K = \Delta H - T \Delta S, \quad (3)$$

where R is the gas constant (8.314 J K $^{-1}$ mol $^{-1}$) and T is the absolute temperature during the interaction in Kelvin degrees.

2.5 | Preparation of β -lap:SBE- β -CD inclusion complex

The inclusion complex of β -lap:SBE- β -CD was prepared using an excess of β -lap in a glass vial with 5 mL of 1.5% SBE- β -CD solution prepared in a phosphate buffer (0.05 M, pH = 7.4) under magnetic stirring 300 rpm during 24 hours at $25 \pm 1^\circ\text{C}$. The yellowish dispersion was centrifuged at 8792 g for 15 minutes and the supernatant filtered through a 0.22- μm membrane filter (Millex, Millipore, France). The sample was frozen at -80°C for 24 hours and freeze-dried (FTSsystems Model EZ-Dry, New York) for 36 hours prior to characterization studies of the inclusion complex.

2.6 | Characterization of β -lap:SBE- β -CD inclusion complex

2.6.1 | Fourier transform infrared spectroscopy

Fourier transform infrared spectra were recorded in a Vertex 70 (Bruker Optics, Ontario, Canada) spectrometer equipped with a DTGS detector, a Globar source and a wide-range beam splitter, using a single-reflection diamond attenuated total reflectance accessory (Platinum, Bruker Optics, Ontario, Canada). The IR spectra were obtained at a 2 cm^{-1} resolution in the region of 4000 to 600 cm^{-1} .

2.6.2 | X-ray powder diffraction

X-ray powder diffractograms were obtained using a D8 Advanced Bruker AXS, equipped with a theta/theta goniometer, operating in the Bragg-Brentano geometry with a fixed specimen holder, Cu K α (0.15419 nm) radiation source and a LynxEye detector. The voltage and electric current applied were 40 kV and 40 mA , respectively. The opening of the slit used for the beam incident on the sample was 0.6 mm . The sample was scanned within the scan range of $2\theta = 5^\circ$ to 50° continuous scan, with a scan rate of $2\text{ deg}\cdot\text{min}^{-1}$.

2.6.3 | Thermal analysis

Thermogravimetric (TG) and differential scanning calorimetry curves were obtained using simultaneous thermal analysis equipment (Jupiter STA 449, Netzsch). Samples of around 5 mg were placed in sealed aluminum crucibles with pierced lids. Measurements were made from room temperature up to 400°C using a heating rate of $10^\circ\text{C}/\text{min}$. The sensors and crucibles were under a constant flow of nitrogen ($70\text{ mL}\cdot\text{min}^{-1}$) during the experiment.

2.6.4 | NMR experiments

Proton nuclear magnetic resonance (^1H NMR) chemical shifts (δ) and 2D ROESY (rotating frame nuclear Overhauser effect spectroscopy) experiments were performed using a Varian 400 MHz NMR spectrometer (Santa Clara, California) operating at 298.1 K . For NMR analysis, samples (β -lap, SBE- β -CD, and β -lap:SBE- β -CD inclusion complex) were dissolved in a 5-mm tube D_2O for 12 hours at 25°C . Sodium 3-(trimethylsilyl) propionate- d_4 was used as an internal chemical shift reference for ^1H NMR spectra. Each spectrum consisted of 64 scans with a spectral width of 6410.3 Hz , an acquisition time of 2.556 seconds , and a recycle delay of 2 seconds per scan. The pulse angle was 90° . 2D-ROESY experiments were recorded at a spin lock of 600 milliseconds .

2.7 | Molecular modeling of the β -lap:SBE- β -CD inclusion complex

Molecular modeling was used to elucidate the specific aspects of intermolecular interaction and calculate the interaction energy between β -lap and SBE- β -CD. There are several reports in the literature using molecular modeling of drugs in CD inclusion complexes.^{11,24-26} To address the synthesis of CD derivatives, the following considerations were taken into account: (i) The regioselectivity of the reaction occurs mainly in the primary hydroxyl group OH (6), since this is the most accessible, followed by the secondary hydroxyl OH (2) with the highest acidity ($\text{pK}_a = 12.2$)²⁷; (ii) the formation of homologous

derivatives with the lowest and highest molar substitution (MS) ratios²⁸ were also obtained in addition to the product.²⁷

Our approach was to construct 1000 structures (40 configurations with 25 different conformations, each) for the SBE- β -CD, starting from the tridimensional structure of the β -cyclodextrin (β -CD).²⁹ The 40 configurations were built considering both aspects of synthesis mentioned above. Regarding the MS ratio of 0.9, it seems reasonable to assume that the SBE- β -CD structure (7 glucose units) has, on average, 6 SBE units. Thus, 20 configurations were built with 6 SBE units, 10 with 5 SBE units and 10 with 7 SBE units. For each SBE unit added during the construction of the structures, the following probability rates of the substitutional positions were considered: 70% for OH (6), 20% for OH (2), and 10% for OH (3), for the substitutional positions. The conformer search was performed using Genetic Algorithm and Energy Score Function available in the OpenBabel library,³⁰ with default convergence parameters. The geometry optimizations for all 1000 structures were computed using MMFF94s force field.³¹ Next, the values of intermolecular interaction energy for host:guest inclusion complexes were calculated using Autodock VINA software,³² considering the entire host structure as the active site with the exhaustiveness parameter set to 8. All the molecular modeling methodology was performed in an automated fashion, using the CycloMolder platform.

2.8 | Statistical analysis

All experiments were performed in triplicate, and the results expressed as the mean \pm SD. The means of 2 groups were compared using nonpaired Student's t tests. When comparing multiple groups, one-way analysis of variance (ANOVA) was applied with the Tukey multiple comparison procedure. The statistical data were considered significant at $P < .05$.

3 | RESULTS AND DISCUSSION

This work set out to study the interaction energy mechanism involved in the binding between β -lap and CD cavities. Supramolecular inclusion complexes were obtained by interaction between β -lap and aqueous solution containing CDs (β -, HP- β -, SBE- β -, γ -, and HP- γ -CD). The supramolecular complex presenting the most favorable energy interaction determined by ITC was characterized using spectroscopy and thermal analyses. In the final step, molecular modeling was traced to elucidate the chemical groups involved in the binding of β -lap enclosed into SBE- β -CD hydrophobic cavity.

3.1 | Solubility study of the β -lap in CD supramolecular complexes

The use of CD represents an interesting strategy for the enhancement of β -lap aqueous solubility. The influence of the CD cavity size (β - and γ -CDs) and the hydrophilization of CD by chemical substitution (HP- β -, SBE- β -, and HP- γ -CDs) on the apparent solubility of β -lap in aqueous medium was evaluated using phase solubility diagrams.²³ Figure 2 shows the phase diagrams of β -lap with 5 different types and concentrations of CDs in phosphate buffer (0.05 M pH = 7.4). In

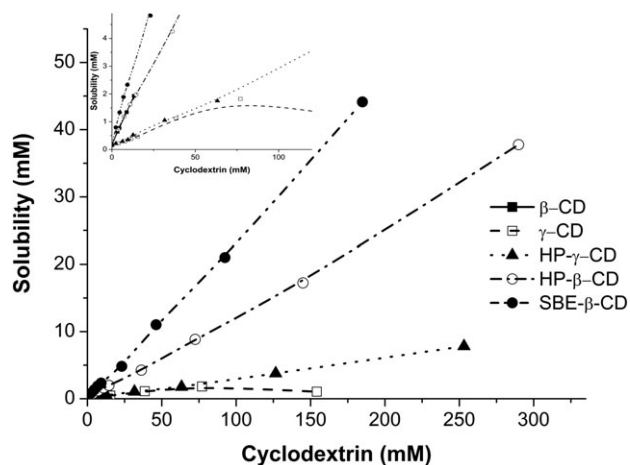


FIGURE 2 Experimental phase solubility diagram of β -lap for β -CD (■), HP- β -CD (○), SBE- β -CD (●), γ -CD (□), and HP- γ -CD (▲) at pH 7.4 ($n = 3$)

general, the solubility of β -lap increased for all CDs tested and was highly dependent on the type and concentration of the CDs. The aqueous solubility of β -lap increased linearly as a function of β -, HP- β -, SBE- β -, and HP- γ -CDs concentrations. Linearity ($R^2 > 0.99$) was characteristic of the A_L -type system and suggested that water-soluble complexes are formed in solution (Table 2). The γ -CD presented a typical B_5 -type solubility curve above 80 mM with a significant decrease in β -lap solubility (Figure 2). The B_5 -type solubility curve denotes an initial rise in the solubility of the β -lap followed by a plateau and a decreasing region resulting from the formation of poorly water-soluble inclusion complexes. The ascending B_5 -type curve showed a linear profile ($R^2 = 0.992$).

Slopes values of 0.1306, 0.1281, 0.2363, 0.0224, and 0.0303 were obtained for β -, HP- β -, SBE- β -, γ -, and HP- γ -CD, respectively. Because the straight line had a slope less than unity, it was assumed that the increase in solubility was due to the formation of a 1:1 stoichiometry complex between the guest (β -lap) and host molecules (CDs). In this connection, assuming that 1:1 complexes were formed, the apparent stability constants ($K_{1:1}$) of the binary complexes were calculated (Table 2). The $K_{1:1}$ values appeared in the following order: SBE- β -CD > HP- β -CD > β -CD > HP- γ -CD > γ -CD, indicating the greater affinity of modified CD with β -lap compared to those parent β - and γ -CDs. The solubility constants found in the present study were almost identical to that previously reported for β -lap:HP- β -CD ($K_{1:1} = 0.961 \times 10^3 \text{ M}^{-1}$, DS = 0.7),¹¹ for β -lap:HP- β -CD ($K_{1:1} = 0.94 \times 10^3 \text{ M}^{-1}$) and β -lap: γ -CD ($K_{1:1} = 0.16 \times 10^3 \text{ M}^{-1}$),¹² and for β -lap: β -CD ($K_{1:1} = 0.996 \times 10^3 \text{ M}^{-1}$) and β -lap:SBE- β -CD

($K_{1:1} = 1.122 \times 10^3 \text{ M}^{-1}$, DS = 1.0).²¹ It is noteworthy that β -lap:HP- γ -CD complex had not been evaluated in previous studies. $K_{1:1}$ variations can be explained by pH difference between the aqueous media and the degree of substitution of the CDs studied by the authors. In the present study, SBE- β -CD appears to be a significantly better host molecule for β -lap complexation. This CD shows $K_{1:1}$ value twofold higher than with the other β -CD derivate and tenfold higher than with γ -CD molecules. The appropriate cavity diameter of β -CDs (~6 Å, Table 1) facilitates molecular recognition between host-guest molecules compared to γ -CDs (~8 Å). The best performance of modified CDs compared to their parent β - and γ -CDs could be explained due the presence of substituents increasing the hydrophobic region of the CD cavity, thus favoring and stabilizing the inclusion complexation of the β -lap in the hydrophobic guest molecule.³³ Therefore, cavity size and type of the CD molecule are important parameters that influenced the formation of the β -lap:CD complex.

The CE of β -lap into CD solution was higher for SBE- β -CD, thus confirming the best affinity of the β -lap:SBE- β -CD inclusion complex. The CE value of β -lap into SBE- β -CD solution of 0.309 indicated that approximately only 1 out of every 4 CD molecules forms a complex with the drug (molar ratio of 1:4), assuming a 1:1 drug/CD complex formation. According to Loftsson et al, if CE is 0.1 then 1 out of every 11 CD molecules forms a complex with the drug, while a CE of 0.01 indicates that only 1 out of every 100 CD molecules forms such a complex.¹⁸

The aqueous solubility of β -lap in CD complexes was significantly higher than that of the pure drug in distilled water (Figure 3). Solubility of β -lap was increased 12-, 10.1-, and 11.8-fold for 1.5% (w/w) of β -, HP- β -, and SBE- β -CDs at 25°C, respectively. Solubility enhancement was very poor when using γ -CD (2.2-fold) and HP- γ -CD (2.4-fold). Highly water-soluble chemically modified CDs (HP- β -, SBE- β -, and HP- γ -CDs) used at concentrations of up to 40% (w/w) lead to considerably higher solubility enhancements (236-, 276-, and 49-fold, respectively) compared to their parent β - and γ -CDs (Figure 2).

Further, the effect of the pH of the medium on the apparent solubility of β -lap solubilization was investigated using SBE- β -CD at a fixed concentration of 6.93 mM. The solubility enhancement of β -lap in the pH medium between 5.5 and 8.0 containing SBE- β -CD increased 12-fold (from 0.16 to 1.97 mM). Obviously, this effect was attributed not to drug ionization, but to the aqueous medium of SBE- β -CD.

3.2 | The ITC experiments: thermodynamic analysis

To study the thermodynamics of binding interactions of β -lap and CDs, ITC experiments were performed in phosphate buffer (0.05 M pH = 7.4) at 25°C. Data were corrected from dilution effects and led to

TABLE 2 Apparent stability constants ($K_{1:1}$), complexation efficiency (CE), and molar ratio obtained from phase solubility diagrams of β -lap in CDs

Cyclodextrin	Slope (S_0)	Correlation Coefficient (R^2)	$K_{1:1}$ ($\times 10^3 \text{ M}^{-1}$)	CE	Drug:CD Molar Ratio
β -CD	0.1285	0.999	0.918	0.147	1:8
HP- β -CD	0.1319	0.998	0.950	0.152	1:8
SBE- β -CD	0.2363	0.999	1.934	0.309	1:4
γ -CD	0.0224	0.992	0.143	0.023	1:45
HP- γ -CD	0.0303	0.998	0.195	0.031	1:33

CDs in pH = 7.4, phosphate buffer (0.05 M) at 25°C

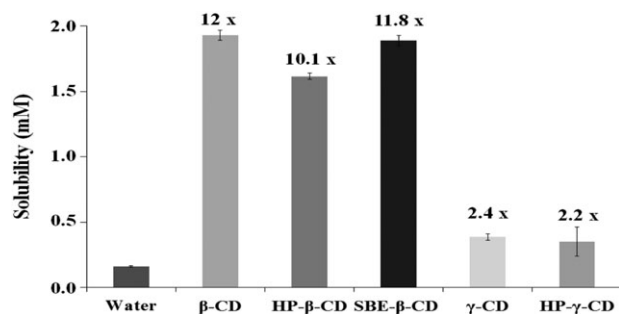


FIGURE 3 Apparent solubility of β -lap in 1.5% (w/w) β -, HP- β -, SBE- β -, γ -, and HP- γ -CD solutions at molar concentrations of 13.22, 10.87, 6.93, 11.57, and 9.49 mM, respectively (pH 7.4 and 25°C)

differential binding curves. A representative calorimetric titration profile of the binding of β -lap (0.16 mM) to SBE- β -CD (6.93 mM) is shown in Figure 4. Each peak in the binding isotherm (Figure 4A) represents a single injection of the β -lap into the CDs solution. Exothermic heat flows, which were released after successive injections of 2- μ L aliquots of SBE- β -CD into a sample cell containing β -lap, were

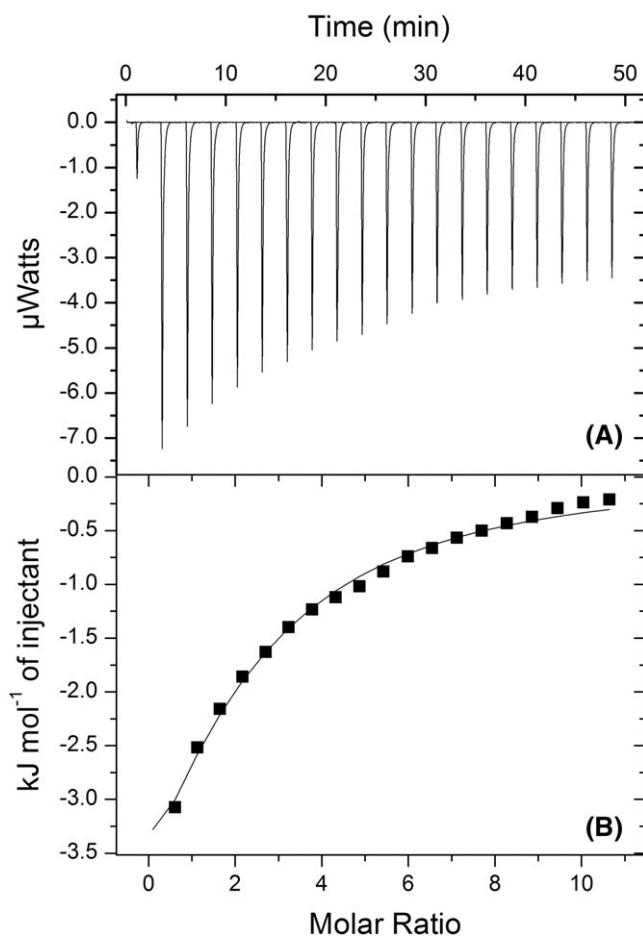


FIGURE 4 A, Typical ITC data corresponding to the binding interaction of 6.93 mM of SBE- β -CD with 0.16 β -lap at pH 7.4 and 25°C. Exothermic heat flows occurring upon successive injection of 2- μ L aliquots of SBE- β -CD into sample cell containing β -lap. B, Integrated heat profile of the calorimetric titration. The solid line represents the best nonlinear least squares fit to a single binding site model. Heat flows accounting for dilution effects of the CD solution in the buffer solution only were further subtracted from each experimental heat flow

integrated and expressed as a function of the molar ratio between the 2 reactants (Figure 4B).

The ITC integrated heat data profiles obtained for the binding interaction between β -lap and β -, HP- β -, SBE- β -, γ -, and HP- γ -CDs are shown in Figure 5. A standard nonlinear least squares regression-binding model based on the one-site binding model (1:1) was used to determine the stoichiometry of the interaction (n), binding constant (K), change in enthalpy (ΔH), entropy (ΔS), and Gibbs free energy (ΔG) released upon the interaction between β -lap and CDs.

Table 3 shows the corresponding thermodynamic parameters of the ITC integrated heat interaction data between β -lap and CDs. The stoichiometry of interaction presented a high molar ratio for γ -CD (5.5) compared to other CDs, indicating a greater ability to accommodate β -lap in their cavities. This effect is associated with the direct insertion of the drug into the γ -CD cavity formed by 8 glucose units that present top to bottom diameters with a cavity corresponding to 7.5 to 8.3 Å and volume of 427 Å³ (Table 1).

The values of binding constant K showed that much higher affinities and much stronger interactions were obtained for SBE- β -CD ($K = 4160 \text{ M}^{-1}$) compared to other CDs (K varies from 2300 to 3080 M^{-1}). All CDs showed favorable enthalpy changes indicating that the interaction process of the β -lap with CD, leading to complex formation, is exothermic. However, looking at the results, the complexation of β -CD and derivatives with β -lap are seen to be more exothermic than that of γ -CD. The interaction between a guest drug and a CD cavity is stronger and the stability of the complex is higher

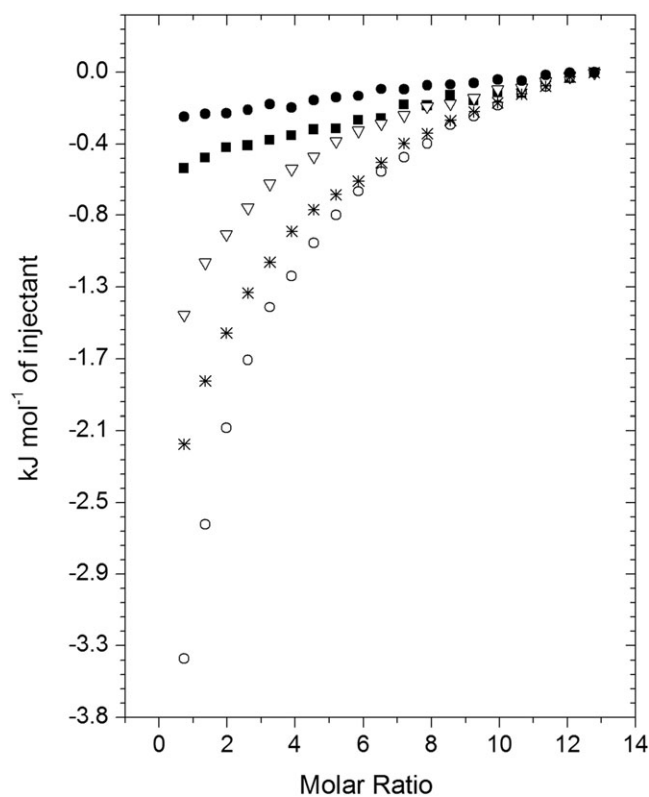


FIGURE 5 Binding interaction between β -lap and β -CD (\circ), HP- β -CD (∇), SBE- β -CD ($*$), γ -CD (\blacksquare), and HP- γ -CD (\bullet) at molar concentrations of 13.22, 10.87, 6.93, 11.57, and 9.49, respectively. Injections of 2 μ L of CD solutions were made in a 0.16 mM β -lap in phosphate buffer (0.05 M) at pH 7.4 and temperature fixed at 298 K (25°C)

TABLE 3 Stoichiometry (*n*), binding constant (*K*), enthalpy (ΔH), entropy ($T\Delta S$), and Gibbs free energy (ΔG) of binding of β -lap with CDs at pH 7.4 according to a single binding site model

Sample	<i>n</i> ^a	<i>K</i> ^b (M ⁻¹)	ΔH ^c (kJ·mol ⁻¹)	$T\Delta S$ ^d (kJ·mol ⁻¹)	$\Delta G = \Delta H - T\Delta S$ ^e (kJ·mol ⁻¹)
β -CD	1.8	3065	-6.58	13.32	-19.90
HP- β -CD	2.5	2580	-2.76	16.73	-19.49
SBE- β -CD	2.4	4160	-4.92	15.74	-20.66
γ -CD	5.5	3080	-0.55	19.38	-19.93
HP- γ -CD	3.3	2300	-0.23	18.96	-19.19

^aStandard deviations in *n* are less than 2%.

^bErrors in *K* values ranged from 1% to 8%.

^cErrors in ΔH ranged from 1 to 7%.

^dErrors in $T\Delta S$ are 1% to 4%.

^eErrors in ΔG are less than 2%.

when binding affinity constants are higher and when ΔH is more exothermic.³⁴ Favorable enthalpy is derived from new interactions, such as hydrophobic ones, associated with the displacement of the water molecules from the cavity of the CD by the more hydrophobic ligand. Furthermore, the gain in the number of hydrogen bonds, Van der Waals, and electrostatic interactions between the molecules may still result in higher favorable enthalpy. Van der Waals interactions are maximized by a perfect geometric fit between drug and target, while the strength of the hydrogen bonds is greatest when the distance and angle between acceptors and donors are optimal.³⁵ γ -CD and HP- γ -CD showed enthalpy close to zero, indicating that distance and angle of the host-guest are suboptimal where the interactions are less favorable. This means therefore the stronger Van der Waals, hydrogen bonds, or electrostatic interactions also take place during the interaction between β -CD and its derivate with β -lap compared with γ -CD.

Entropy can be described as a measure of disorder within a system, as well as the energy state of a system. The entropy effects ($T\Delta S$) of the host-guest complexes were all positive. γ -CD and its derivate showed high entropy values. Favorable desolvation entropy is the predominant force associated with the binding energy of hydrophobic groups.³⁶ Thus, the positive entropy effect can be attributed to the breakdown of water structure around β -lap, which promotes drug transfer from the aqueous medium to a more apolar site (CDs cavity), releasing water molecules from the CD cavity. The plot of ΔH vs $T\Delta S$ shows a linear dependence with slope = 0.866 ± 0.02 and correlation coefficient $R^2 = 0.97$ (Figure 6). This suggests enthalpy-entropy compensation, and this correlation indicates the significance of solvent reorganization during the binding process.^{35,37}

Gibbs free energy change (ΔG) is the most important energetic parameter measured by ITC. ΔG indicates that the formation of host-guest inclusion complexes in aqueous solution is a spontaneous process, with more negative values of ΔG favoring higher affinity binding. The stability of β -lap:CDs was better with SBE- β -CD. Thus, the inclusion complexation of β -lap:CD is predominantly governed by hydrophobic interactions driven by entropy energy. However, the enthalpy of β -CD and its derivate contributes to greater binding affinity to β -lap for the formation and stabilization of the inclusion complex.

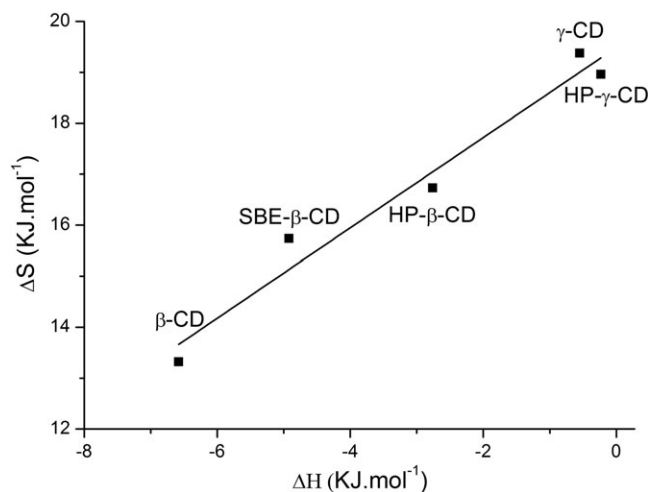


FIGURE 6 Enthalpy-entropy compensation plot corresponding to inclusion complex formation of β -lap (0.16 mM) with CDs at 25°C

3.3 | Characterization of the inclusion complex

Characterization of the inclusion complex was performed to obtain further information on β -lap:SBE- β -CD, which showed a better host-guest formation in aqueous solution.

The XRD shows the X-ray powder patterns of the raw materials, the physical mixture, and the inclusion complex (Figure 7). The β -lap powder pattern is characterized by a sharp and intense peak at 9.5°, and secondary peaks at 15.3°, 19.4°, and 26.4°, in agreement with the crystalline structure reported by Cunha-Filho et al.³⁸ On the other hand, SBE- β -CD exhibits the broad bumps associated with its amorphous form, albeit with the presence of some residues of crystalline K_2HPO_4 . The most intense peak of β -lap clearly indicates the presence of this compound in the physical mixture, but this is not observed in the final sample, supporting the hypothesis of the production of an inclusion complex.

Similar conclusions can be drawn by analyzing the differential scanning calorimetry/TG thermal analysis results presented in Figure 8. The melting point of β -lap is clearly defined by a sharp endothermic peak with an onset temperature of 153°C, whereas the dehydration of SBE- β -CD is observed as a broad band around 100°C. The β -lap fusion peak still fingerprints the presence of the crystalline

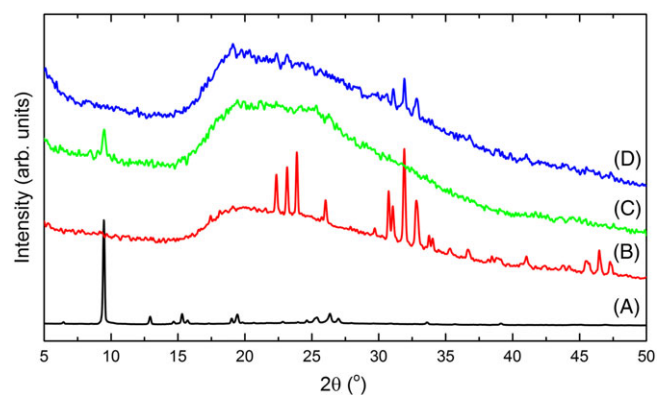


FIGURE 7 X-ray powder patterns of A, β -lap, B, SBE- β -CD, C, the physical mixture, and D, the inclusion complex

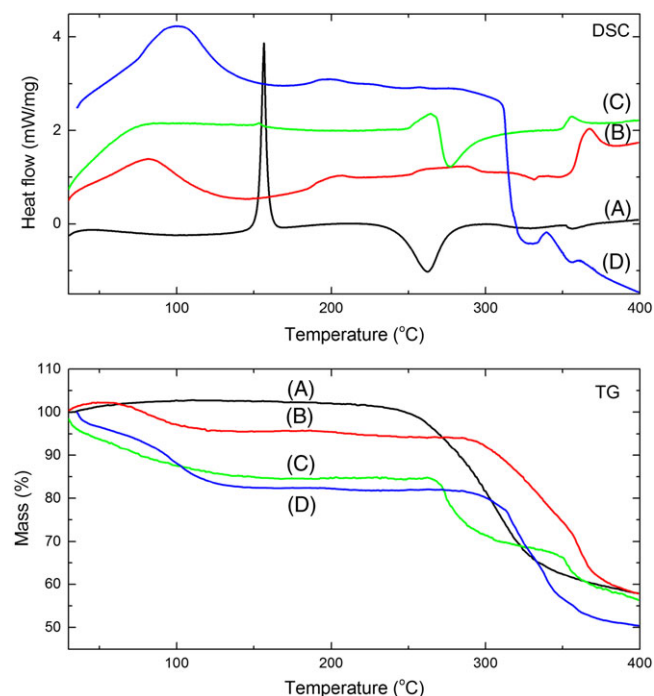


FIGURE 8 Differential scanning calorimetry (DSC) and thermogravimetric (TG) curves of A, β -lap, B, SBE- β -CD, C, the physical mixture, and D, the inclusion complex (d)

form of this compound in the physical mixture, but the absence of this peak in the final product is evidence of the formation of an inclusion complex.^{39,40} The TG curves show 2 different regimes: below 100°C the dehydration process is observed, while above 270°C the mass loss processes are associated with the decomposition of the investigated samples.

The above mentioned characterization methods are able to confirm that no crystalline β -lap is present in the final product but cannot verify the formation of the inclusion complex. To shed some light on this, the samples were investigated using infrared spectroscopy (Figure 9). The infrared spectrum peaks of β -lap are in close agreement with those reported in the literature,^{21,39} thus confirming the chemical identity of the sample. Furthermore, the physical mixture can be directly interpreted as the simple combination of both spectra, but there is a large overlap of the corresponding bands. The most intense bands of β -lap are weakly observed in the infrared spectrum of the physical mixture, but they are in the same positions as in the raw material, showing no evidence of the intermolecular interactions, as observed in the insert of Figure 9. These bands can be approximately classified as the stretching modes of the C=O (1694 cm^{-1}) and aromatic ring ($1643, 1633, 1598, \text{ and } 1569\text{ cm}^{-1}$) double bonds. On the other hand, in the final product, it is possible to observe the same bands, but wider and slightly shifted, evidencing the presence of β -lap and the loss of the crystalline structure confirming to the formation of the inclusion complex.

The chemical groups of β -lap involved in the intermolecular and intramolecular interactions with SBE- β -CD cavity were then studied by 2D ROESY (Figure 10). This experiment allowed observation of the spatial proximity at the 5 Å maximal limit among the functional groups of the β -lap and hydrogen protons present in the cavity and chain of the SBE- β -CD. The circle cross peak coincided with the

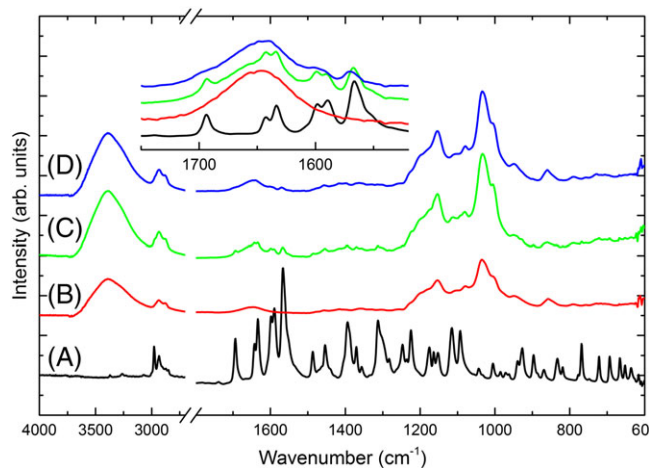


FIGURE 9 Infrared spectra of A, β -lap, B, SBE- β -CD, C, the physical mixture, and D, the inclusion complex

intermolecular interactions between the hydrogen of β -lap and the chain and internal cavity hydrogens of the SBE- β -CD. The NMR spectrum of complexes showed no new peaks, but some changes in the chemical shifts occurred, casting light on the interaction, position, and orientation of the guest molecule. The ROESY spectrum confirms the interaction between β -lap and SBE- β -CD, 4 NOEs of which prove the proximity of the protons. H_d in benzene moiety and H_c in 2,2-dimethyl-pyran moiety from β -lap interact with the H_3 proton of SBE- β -CD. These results corroborate other studies using β -lap in different CD inclusion complexes.^{11,12} Additionally, H_a and H_b protons from β -lap showed cross peak correlations with H_4' and H_2' H_3' of SBE- β -CD, respectively, suggesting that β -lap is covered by the chain of SBE- β -CD during its inclusion inside the complex cavity. These data demonstrate the penetration of β -lap into the SBE- β -CD cavity as well as a simultaneous form of interaction with the chain regions of the CD.

3.4 | Molecular modeling calculations of the β -lap: SBE- β -CD

The molecular docking results showed 2 main orientations regarding the position of the guest molecule (β -lap) included in the host molecule (SBE- β -CD). The first, known as orientation I, has the benzene moiety at the wider rim of the SBE- β -CD, and the other, known as orientation II, has the 2,2-dimethyl-pyran moiety at the wider rim. The average docking energy for the first 10 best solutions, considering orientation I, is -7.0 kcal/mol . On the other hand, the average energy of the first 10 best solutions for orientation II is -6.8 kcal/mol . The overall best solution for orientation I is shown in Figure 11A, with a docking energy of -7.2 kcal/mol , while the overall best docking solution for orientation II can be found in Figure 11B, with an energy of -7.0 kcal/mol . The best solution for orientation I is stabilized by several hydrophobic contacts and by 2 hydrogen bonds (3.03 and 3.04 \AA), while the best solution for orientation II is also stabilized by several hydrophobic contacts and by 2 hydrogen bonds (2.91 and 3.31 \AA), one of which, however, very long (3.31 \AA) and, therefore, less stable. The final molecular modeling results reveal that orientation I is the most stable, in general, and probably occurs more frequently than orientation II, for the β -lap:

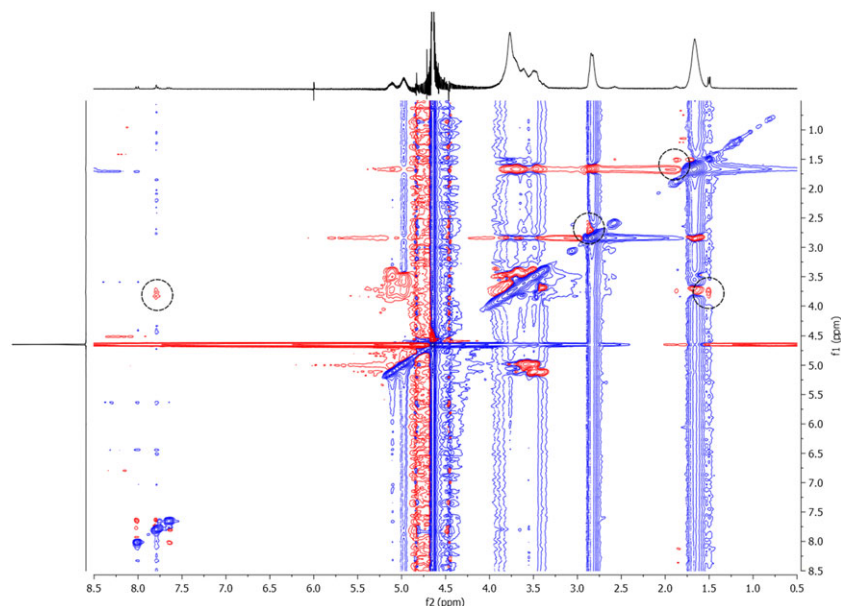


FIGURE 10 Expansion of the contour ROESY spectrum of the β -lap:SBE- β -CD inclusion complex (400 MHz, D₂O)

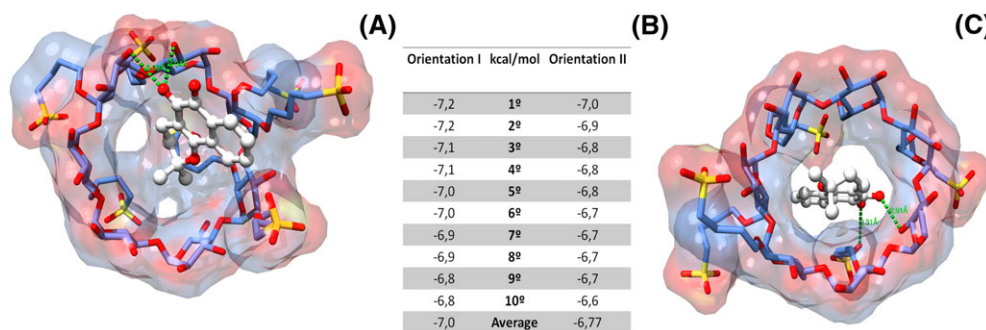


FIGURE 11 Summary of the molecular docking results. A, Best docking solution for orientation I. B, Table with the binding energies (kcal/mol) of the 10 best docking solutions for each orientation. C, Best docking solution for orientation II. Dashed lines represent intermolecular hydrogen bonds between host (SBE- β -CD) and guest (β -lap) molecules

SBE- β -CD inclusion complex. The importance of the carbonyl groups present in β -lap should be emphasized, as well as their contribution to the stabilization of the β -lap:SBE- β -CD inclusion complex, particularly by the formation of these intermolecular hydrogen bonds.

4 | CONCLUSION

In this work, the nature of the supramolecular interactions between β -lap with CDs (β -, HP- β -, SBE- β -, γ -, and HP- γ -CD) was investigated using phase solubility and isothermal titration calorimetry (ITC). Among the 5 CDs studied, SBE- β -CD was the best host molecule for β -lap complexation, resulting in an A_L-type phase-diagram with a high apparent stability constant. Furthermore, SBE- β -CD showed high affinity and strong binding interaction with β -lap through spontaneous and exothermic complexation, predominantly governed by hydrophobic interactions driven by entropy energy. The physicochemical analyses of the complexes confirmed the penetration of β -lap into the SBE- β -CD cavity with loss of the drug crystalline structure conforming the formation of an amorphous inclusion complex. The molecular docking results showed 2 main orientations. The best orientation showed the benzene moiety from β -lap at the wider rim of the SBE- β -CD, stabilized by

several hydrophobic interactions and by 2 hydrogen bonds. In conclusion, thermodynamic profile and molecular modeling calculations elucidated the formation of a stable β -lap:SBE- β -CD inclusion complex, which is proposed as an approach for use in drug delivery systems.

ACKNOWLEDGEMENTS

The authors thank the Brazilian Research Agencies for their financial support: CAPES (under graduated program), CNPq (National Council for Research and Development of Brazil, grants 311232/2013-2; 402282/2013-2), FACEPE (Fundação de Amparo à Ciência e Tecnologia do Estado de Pernambuco, grant APQ-1868-4.03/13), and the Brazilian Ministry of Science and Technology (Ministério da Ciência, Tecnologia e Inovação - MCTI).

REFERENCES

- Burnett AR, Thomson RH. Lapachol. *Chem Ind.* 1968;50:1771
- Aires AL, Ximenes ECPA, Barbosa VX, Góes AJS, Souza VMO, Albuquerque MCPA. β -lapachone: a naphthoquinone with promising antischistosomal properties in mice. *Phytomedicine.* 2014;21:261-267.
- Eyong KO, Kumar PS, Kuete V, Folefoc GN, Nkengfack EA, Baskaran S. Semisynthesis and antitumoral activity of

- 2-acetylfuranonaphthoquinone and other naphthoquinone derivatives from lapachol. *Bioorg Med Chem Lett*. 2008;18:5387-5390.
4. Li LS, Bey EA, Dong Y, et al. Modulating endogenous NQO1 levels identifies key regulatory mechanisms of action of β -lapachone for pancreatic cancer therapy. *Clin Cancer Res*. 2001;17:275-285.
 5. Ough M, Lewis A, Bey EA, et al. Efficacy of β -lapachone in pancreatic cancer treatment: exploiting the novel, therapeutic target NQO1. *Cancer Biol Ther*. 2005;4:95-102.
 6. Pardee AB, Li YZ, Li CJ. Cancer therapy with beta-lapachone. *Curr Cancer Drug Targets*. 2002;2:227-242.
 7. Planchon SM, Wuerzberger S, Frydman B, et al. Beta-lapachone-mediated apoptosis in human promyelocytic leukemia (HL-60) and human prostate cancer cells: a p53-independent response. *Cancer Res*. 1995;55:3706-3711.
 8. Yamashita M, Kaneko M, Tokuda H, Nishimura K, Kumeda Y, Iida A. Synthesis and evaluation of bioactive naphthoquinones from the Brazilian medicinal plant, *Tabebuia avellanedae*. *Bioorg Med Chem*. 2009;17:6286-6291.
 9. Reinicke KE, Bey EA, Bentle MS, et al. Development of beta-lapachone prodrugs for therapy against human cancer cells with elevated NAD(P)H: quinone oxidoreductase 1 levels. *Clin Cancer Res*. 2005;11:3055-3064.
 10. Wuerzberger SM, Pink JJ, Planchon SM, Byers KL, Bornmann WG, Boothman DA. Induction of apoptosis in MCF-7:WS8 breast cancer cells by beta-lapachone. *Cancer Res*. 1998;58:1876-1885.
 11. Cavalcanti IM, Mendonça EA, Lira MC, et al. The encapsulation of β -lapachone in 2-hydroxypropyl- β -cyclodextrin inclusion complex into liposomes: a physicochemical evaluation and molecular modeling approach. *Eur J Pharm Sci*. 2011;44:332-340.
 12. Nasongkla N, Wiedmann AF, Bruening A, et al. Enhancement of solubility and bioavailability of β -lapachone using cyclodextrin inclusion complexes. *Pharm Res*. 2003;20:1626-1633.
 13. Carrier RL, Miller LA, Ahmed I. The utility of cyclodextrins for enhancing oral bioavailability. *J Control Release*. 2007;123:78-99.
 14. Duan MS, Zhao N, Ossurardottir IB, Thorsteinsson T, Loftsson T. Cyclodextrin solubilization of the antibacterial agents triclosan and triclocarban: formation of aggregates and higher-order complexes. *Int J Pharm*. 2005;297:213-222.
 15. Duchene D, Bochot A. Thirty years with cyclodextrins. *Int J Pharm*. 2016;514:58-72.
 16. Loftsson T, Duchene D. Cyclodextrins and their pharmaceutical applications. *Int J Pharm*. 2007;329:1-11.
 17. Loftsson T, Brewster ME. Pharmaceutical applications of cyclodextrins: effects on drug permeation through biological membranes. *J Pharm Pharmacol*. 2001;63:1119-1135.
 18. Loftsson T, Brewster ME. Pharmaceutical applications of cyclodextrins: basic science and product development. *J Pharm Pharmacol*. 2010;62:1607-1621.
 19. Messner M, Kurkov SV, Jansook P, Loftsson T. Self-assembled cyclodextrin aggregates and nanoparticles. *Int J Pharm*. 2010;387:199-208.
 20. Sousa FB, Denadai AM, Lula IS, et al. Supramolecular self-assembly of cyclodextrin and higher water soluble guest: thermodynamics and topological studies. *J Am Chem Soc*. 2008;130:8426-8436.
 21. Cunha-Filho MS, Marinho BC, Labandeira JJT, Pacheco RM, Landin M. Characterization of β -lapachone and methylated- β -cyclodextrin solid-state systems. *AAPS PharmSciTech*. 2007;8:E60
 22. Wang F, Blanco E, Ai H, Boothman DA, Gao J. Modulating beta-lapachone release from polymer millirods through cyclodextrin complexation. *J Pharm Sci*. 2006;95:2309-2319.
 23. Higuchi T, Connors KA. Phase solubility techniques. *Adv Anal Chem Instrum*. 1965;4:117-212.
 24. Mendonça EA, Lira MC, Rabello MM, et al. Enhanced antiproliferative activity of the new anticancer candidate LPSF/AC04 in cyclodextrin inclusion complexes encapsulated into liposomes. *AAPS PharmSciTech*. 2012;13:1355-1366.
 25. Miletic T, Kyriakos K, Graovac A, Ibric S. Spray-dried voriconazole-cyclodextrin complexes: solubility, dissolution rate and chemical stability. *Carbohydr Polym*. 2013;98:122-131.
 26. Silva CV, Barbosa JA, Ferraz MS, et al. Molecular modeling and cytotoxicity of diffractaic acid: HP-beta-CD inclusion complex encapsulated in microspheres. *Int J Biol Macromol*. 2016;92:494-503.
 27. Wenz G. Cyclodextrins as building blocks for supramolecular structures and functional units. *Angew Chem Int Ed Engl*. 1994;33:803-822.
 28. Treib J, Baron JF, Grauer MT, Strauss RG. An international view of hydroxyethyl starches. *Intensive Care Med*. 1999;25:258-268.
 29. Saenger W, Jacob J, Gessler K, et al. Structures of the common cyclodextrins and their larger analogues beyond the doughnut. *Chem Rev*. 1998;98:1787-1802.
 30. O'Boyle NM, Banck M, James CA, Morley C, Vandermeersch T, Hutchison GR. Open Babel: an open chemical toolbox. *J Chem*. 2011;3:1-14.
 31. Halgren TA, MMFF VI. MMFF94s option for energy minimization studies. *J Comput Chem*. 1999;20:720-729.
 32. Trott O, Olson AJ. AutoDock Vina: improving the speed and accuracy of docking with a new scoring function, efficient optimization, and multithreading. *J Comput Chem*. 2010;31:455-461.
 33. Mura P, Furlanetto S, Cirri M, Maestrelli F, Corti G, Pinzauti S. Interaction of naproxen with ionic cyclodextrins in aqueous solution and in the solid state. *J Pharm Biomed Anal*. 2005;37:987-994.
 34. Chaires JB. Calorimetry and thermodynamics in drug design. *Annu Rev Biophys*. 2008;37:135-151.
 35. Freire E. Do enthalpy and entropy distinguish first in class from best in class? *Drug Discov Today*. 2008;13:869-874.
 36. Rekharsky M, Inoue Y, Tobey S, Metzger A, Anslyn E. Ion-pairing molecular recognition in water: aggregation at low concentrations that is entropy-driven. *J Am Chem Soc*. 2002;124:14959-14967.
 37. Sanchez FS, Bouchemal K, Lebas G, Vauthier C, Santos-Magalhães NS, Ponchel G. Elucidation of the complexation mechanism between (+)-usnic acid and cyclodextrins studied by isothermal titration calorimetry and phase-solubility diagram experiments. *J Mol Recognit*. 2009;22:232-241.
 38. Cunha-Filho MS, Landin M, Pacheco RM, Marinho BD. Beta-lapachone. *Acta Crystallogr C*. 2006;62:473-475.
 39. Cunha-Filho MS, Pacheco RM, Landin M. Compatibility of the antitumoral beta-lapachone with different solid dosage forms excipients. *J Pharm Biomed Anal*. 2007;45:590-598.
 40. Mangas-Sanjuan V, Gutiérrez-Nieto J, Echezarreta-López M, et al. Intestinal permeability of β -lapachone and its cyclodextrin complexes and physical mixtures. *Eur J Drug Metab Pharmacokinet*. 2016;41:795-806.

How to cite this article: Xavier-Junior FH, Rabello MM, Hernandez MZ, et al. Supramolecular interactions between β -lapachone with cyclodextrins studied using isothermal titration calorimetry and molecular modeling. *J Mol Recognit*. 2017;30:e2646. <https://doi.org/10.1002/jmr.2646>